Acta Cryst. (1982). A**38**, 454–463

The Kinematical Theory of X-ray Spherical-Wave Diffraction

BY E. V. SHULAKOV AND V. V. ARISTOV

Solid State Physics Institute, Academy of Sciences of the USSR, Chernogolovka, Moscow district, 142432, *USSR*

(*Received* 9 *September* 1980; *accepted* 1 *February* 1982)

Abstract

It is shown that the Fraunhofer approximation, used in the kinematical theory of X-ray diffraction, may fail for a wide variety of crystals with different perfection. The kinematical theory describing the diffraction pattern in the general case is developed. The case of spherical-wave diffraction by a plane parallel crystal is considered in detail. The intensity distribution and the diffraction line width are ascertained to be essentially dependent on the region of diffraction in which the observation plane is located. On the other hand, the diffraction pattern geometry is independent of the diffraction region and is determined only by the crystal structure and the optics of diffraction. The geometry of the diffraction pattern recorded by the divergent-beam method is analysed in detail.

Introduction

General formulations, conclusions and methods of the kinematical theory were developed shortly after the phenomenon of X-ray diffraction by crystals had been discovered, and since then they have remained practically unchanged (see James, 1948; Iveronova & Revkevich, 1978). It follows from the difficulties arising in the analysis of diffraction in the pseudo-Kossel and divergent-beam schemes (Londsdale, 1947) and the development of methods of the dynamical theory of diffraction (Kato, 1961; Afanas'ev & Kohn, 1977) that a more rigorous solution of the problem is necessary and possible. This is because, apart from the assumptions on the character of the interaction of X-ray radiation with matter (the first Born approximation), the Fraunhofer approximation is considered to be valid.

Let us consider which restrictions on the crystal dimensions are imposed by the Fraunhofer approximation. In the first Born approximation the total amplitude of the waves scattered by the crystal may be presented in the form (Cowley, 1975)

$$\psi_{sc}(\mathbf{R}) = A_e \int_{v_c} \psi_0(\mathbf{R}_c)\, \rho(\mathbf{R}_c)\, C_s |\mathbf{R} - \mathbf{R}_c|^{-1} \times \exp(i2\pi K |\mathbf{R} - \mathbf{R}_c|)\, \mathrm{d}^3 R_c. \quad (1)$$

Here $\mathbf{R}$ determines the observation point M (see Fig. 1), $\mathbf{R}_c$ determines the scattering centre position; v_c is the crystal volume; $K = 1/\lambda$, where λ is the wavelength; the coefficient A_e is the Thomson scattering amplitude, $A_e = -e^2/mc^2$, where e is the electron charge, m is the electron mass, c is the velocity of light; C_s is the polarization factor, $C_s = 1$ for σ polarization and $C_s = \mathbf{R}_c.(\mathbf{R} - \mathbf{R}_c)/R_c|\mathbf{R} - \mathbf{R}_c|$ for π polarization; $\psi_0(\mathbf{R}_c)$ describes the incident wave amplitude at the point $\mathbf{R}_c$.

Let us analyse (1) for the case of a spherical incident wave $\psi_0(\mathbf{R}) = R^{-1} \exp(i2\pi KR)$. We choose the vector $\mathbf{R}_1$ on Fig. 1 corresponding to a point b inside the crystal and write $\mathbf{R}_c$ and $\mathbf{R} - \mathbf{R}_c$ in the form $\mathbf{R}_c = \mathbf{R}_1 + \mathbf{r}_c$ and $\mathbf{R} - \mathbf{R}_c = \mathbf{R}_2 - \mathbf{r}_c$, where $\mathbf{R}_2 = \mathbf{R} - \mathbf{R}_1$. Let us assume the crystal dimensions are small as compared with the distances R_1 and R_2, then the expansions for R_c and $|\mathbf{R} - \mathbf{R}_c|$ are

$$R_c \simeq R_1 + \mathbf{s}_1.\mathbf{r}_c + (\mathbf{s}_1 \times \mathbf{r}_c)^2/2R_1$$

$$|\mathbf{R} - \mathbf{R}_c| \simeq R_2 - \mathbf{s}_2.\mathbf{r}_c + (\mathbf{s}_2 \times \mathbf{r}_c)^2/2R_2. \quad (2)$$

Here $\mathbf{s}_1 = \mathbf{R}_1/R_1$ and $\mathbf{s}_2 = \mathbf{R}_2/R_2$. The Fraunhofer approximation means that second-order infinitesimal terms in (2) may be neglected in the calculation of amplitude $\psi_{sc}(\mathbf{R})$.† This can be done, if the relation

$$(\mathbf{s}_1 \times \mathbf{r}_c)^2/R_1 + (\mathbf{s}_2 \times \mathbf{r}_c)^2/R_2 \ll \lambda \quad (3)$$

† An analysis of the X-ray diffraction by crystals of finite dimensions was carried out by Samsonov (1979) taking second-order terms into account in expansion (2).

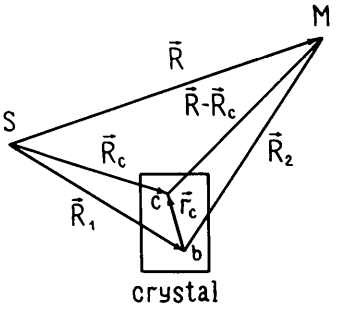

Fig. 1. Geometry of spherical-wave scattering. S is the radiation source, M is the observation point.

0567-7394/82/040454-10$01.00

is satisfied for any point of the crystal $\mathbf{r}_c$. Relation (3) approximately corresponds to the condition: $l \ll l_F = (\lambda R^*)^{1/2}$, where l is the crystal maximum dimension, l_F is the dimension of the first Fresnel zone, $R^* = R_1 R_2/(R_1 + R_2)$. It follows from (3) that the Fraunhofer approximation in the case of the divergent beam (DB) and pseudo-Kossel (PK) methods† fails even for extremely small crystals or blocks ($l_F \gtrsim 0{\cdot}5$ μm and $l_F \gtrsim 0{\cdot}03$ μm, respectively). At $l \gtrsim l_F$ the Fraunhofer diffraction is not realized.‡

This means that there is a wide variety of experimental situations in which the interpretation of the diffraction patterns for imperfect crystals may lead, in the framework of the Fraunhofer approximation, to incorrect results. The Fraunhofer approximation is apparently applicable only to fine-grained polycrystals or strongly deformed single crystals.§

Below, the kinematical theory of spherical-wave diffraction is formulated in the general form. The case of diffraction from a plane parallel crystal plate is considered in detail.

Principles of diffraction pattern formation

In the analysis of spherical-wave diffraction we make use of a representation in terms of the angular spectrum of plane waves (see Born & Wolf, 1968; Kato, 1961). In this case, the crystal response to each of the plane waves forming the spherical wave is determined and the resulting field is calculated by summing all the elementary fields. Such an approach proves to be rather fruitful, since in this way one does not need to state any *a priori* approximation in representing the spherical wave front, and the usual technique of analysis in terms of plane-wave diffraction can be used to its full extent.

1. Angular spectrum of plane waves

The spherical wave $\psi(\mathbf{R}) = R^{-1}\exp(i2\pi KR)$ emitted by a point source has at the point $\mathbf{R}(x,y,z)$ the following Fourier representation:

$$\psi = \int_{-\infty}^{\infty}\int B \exp[i2\pi(px + qy)]\,\mathrm{d}p\,\mathrm{d}q. \qquad (4)$$

† In the DB method the crystal under investigation is placed near an external point source of divergent X-ray radiation. Thereby R_1 is equal to 1–5 mm, $R_2 \gtrsim R_1$. In the PK method the source is excited in the film placed onto the specimen, $R_1 \lesssim 10^{-2}$ mm, $R_2 \gg R_1$.

‡ Notice that as the crystal thickness tends to zero the formulae of the dynamical theory by Kato (1961) are in disagreement with the well-known formulae of kinematical theory (see James, 1948).

§ For example, if ρ_d is the dislocation density, the Fraunhofer approximation is applicable at $\rho_d \gg 1/l_F^2$. The quantitative estimates take the form: $\rho_d \gg 5 \times 10^8$ cm^{-2} and $\rho_d \gg 10^{11}$ cm^{-2} for the DB and PK schemes, respectively; $\rho_d \gg 10^7$ cm^{-2} for diffractometry.

Here $B(p,q,z)$ is the weight function relative to the angular spectrum of the wave $\psi(\mathbf{R})$. We leave the region $p^2 + q^2 = K^2$ out of consideration, regarding the integral in this region as improper. For $p^2 + q^2 \neq K^2$:

$$B = i(K^2 - p^2 - q^2)^{-1/2}\exp[i2\pi(K^2 - p^2 - q^2)^{1/2}|z|]. \qquad (5)$$

The condition $p^2 + q^2 > K^2$ corresponds to surface waves propagating along the plane $z = 0$. The amplitude of these waves decreases rapidly, as $|z|$ increases, and they may be neglected at $|z| \gg \lambda$. The integrand in (4) may be interpreted as uniform plane waves:

$$U(\mathbf{K},\mathbf{R}) = (i/|m|)\exp(i2\pi\mathbf{K}.\mathbf{R}) \qquad (6)$$

provided $p^2 + q^2 < K^2$. Here $\mathbf{K}(p,q,m)$ is the wave vector; λp, λq and λm are the cosines of the angles between the direction $\mathbf{s} = \lambda\mathbf{K}$ of the plane-wave propagation and the coordinate axes X,Y,Z, respectively; $|m| = (K^2 - p^2 - q^2)^{1/2}$. Comparing (6) with (4), (5), one can see that the plane waves under consideration propagate in the half-space $z > 0$ in the positive direction of the Z axis ($m > 0$), and in the half-space $z < 0$ in the negative direction of the Z axis ($m < 0$).

We shall now consider crystal diffraction of the spherical wave $\psi_0(\mathbf{R}) = R^{-1}\exp(i2\pi KR)$ and determine the field of scattered waves in the first Born approximation of diffraction theory.

2. Diffracted wave field

As a result of crystal diffraction, each of the plane waves (6) is transformed, according to (1), into a packet of spherical waves $V(\mathbf{K}_0,\mathbf{R})$:

$$V = A_e\int_{v_c} U_0(\mathbf{K}_0,\mathbf{R}_c)\,\rho(\mathbf{R}_c)\,C_s|\mathbf{R} - \mathbf{R}_c|^{-1} \times \exp(i2\pi K|\mathbf{R} - \mathbf{R}_c|)\,\mathrm{d}^3R_c. \qquad (7)$$

Here $\mathbf{K}_0(p_0,q_0,m_0)$ is the wave vector of the incident plane wave.

Expressing the scattered spherical waves in the integrand of (7) in terms of a spectrum of plane waves (see § 1), we can rewrite formula (7) in the following form:

$$V(\mathbf{K}_0,\mathbf{R}) = W(\mathbf{K}_0,\mathbf{R})U_0(\mathbf{K}_0,\mathbf{R}). \qquad (8)$$

The function $W(\mathbf{K}_0,\mathbf{R})$ in (8) describes a transformation of the plane wave $U_0(\mathbf{K}_0,\mathbf{R})$ due to crystal diffraction and is determined by the expression

$$W = iA_e\int\int_{p_h^2+q_h^2<K^2} |m_h|^{-1}\,C_s f(\mathbf{K}_h - \mathbf{K}_0) \times \exp[i2\pi(\mathbf{K}_h - \mathbf{K}_0).\mathbf{R}]\,\mathrm{d}p_h\,\mathrm{d}q_h. \qquad (9)$$

Here $\mathbf{K}_h(p_h,q_h,m_h)$ is the wave vector of the scattered plane wave, the factor C_s is equal to 1 for σ polarization

and to $\mathbf{s}_0.\mathbf{s}_h$ for π polarization, the function $f(\mathbf{K}_h - \mathbf{K}_0)$ is the Fourier transform of the electron density $\rho(\mathbf{R}_c)$:

$$f = \int_{v_c} \rho(\mathbf{R}_c) \exp[-i2\pi(\mathbf{K}_h - \mathbf{K}_0).\mathbf{R}_c]\, \mathrm{d}^3R_c. \quad (10)$$

The total field of the waves diffracted by the crystal is determined by integration of (8) over p_0 and q_0:

$$\psi_{sc} = \int\int_{p_0^2+q_0^2<K^2} G \exp[i2\pi(p_0 x + q_0 y)]\, \mathrm{d}p_0\, \mathrm{d}q_0. \quad (11)$$

The function $G = B(\mathbf{K}_0,\mathbf{R})\ W(\mathbf{K}_0,\mathbf{R})$ in the integrand determines the angular spectrum of the waves scattered by the crystal. Formula (11) describes a field of diffracted waves in the kinematical approximation of the theory for any geometry of experiment and for an arbitrary distribution $\rho(\mathbf{R}_c)$.

Let us analyse the expressions obtained. For a periodic distribution of the electron density, the function f is different from zero only in a discrete set of regions of reciprocal space. In the case of a homogeneous single crystal this set of regions can be described by a reciprocal lattice (or an averaged one), in which the function f takes on a noticeable value only in the vicinity of the reciprocal-lattice points H.* This means that the wave field $\psi_{sc}(\mathbf{R})$ can be represented as a sum of the fields $\psi_H(\mathbf{R})$ corresponding to different points of the reciprocal lattice. Thereby the diffraction of a plane wave is described in reciprocal space by means of a transformation of the wave vector $\mathbf{K}_0$ into the wave vector $\mathbf{K}_h$ of the scattered wave: $\mathbf{K}_h = \mathbf{K}_0 + \mathbf{H} + \Delta\mathbf{H}$, where $\mathbf{H}$ is the reciprocal-lattice vector and $\Delta\mathbf{H}$ varies in the vicinity of the H point of the reciprocal lattice. Since $|\mathbf{K}_0| = |\mathbf{K}_h| = \lambda^{-1}$ the vectors $\mathbf{K}_0$ and $\mathbf{H}$ are related to each other by the following expression:

$$(\mathbf{H} + \Delta\mathbf{H})^2 + 2\mathbf{K}_0.(\mathbf{H} + \Delta\mathbf{H}) = 0. \quad (12)$$

For a given $\mathbf{K}_0$ (12) determines the H-node section of the reciprocal space by the Ewald sphere. At $\Delta\mathbf{H} = 0$ (12) corresponds to the Bragg equation. The vectors $\mathbf{K}_0$ and $\mathbf{K}_h$ satisfying the Bragg equation will be denoted by $\mathbf{K}_0^B$ and $\mathbf{K}_H^B$.

Let us deterime the field $\psi_H(\mathbf{R})$ corresponding to a fixed value of the vector $\mathbf{H}$.

3. The field of a spherical wave diffracted by a set of crystallographic planes

To find the field $\psi_H(\mathbf{R})$, we take an orthogonal system of coordinates associated with the reciprocal-lattice vector $\mathbf{H}$ and choose the origin of coordinates at the radiation source. Let us direct the Z axis along the vector $-\mathbf{H}$ and set the Y axis in the plane parallel to the crystal surface. The unit vectors along the coordinate axes are determined by the expressions: $\mathbf{e}_x = \mathbf{e}_y \times \mathbf{e}_z$, $\mathbf{e}_y = (\mathbf{n}_0 \times \mathbf{e}_z)/\sin\alpha$, $\mathbf{e}_z = -\mathbf{H}/H$, where α is the angle between the normal to the crystal surface $\mathbf{n}_0$ and $\mathbf{e}_z$ (see Fig. 2). Let us denote the components of the vector $\mathbf{K}_0^B$ as P,Q,M. Let θ be the Bragg angle, and $\Delta P,\Delta Q,\Delta M$ describe a deviation from the vector $\mathbf{K}_0^B$ in the scattering plane. Taking into account that $M = K\sin\theta$, $Q = (K^2\cos^2\theta - P^2)^{1/2}$, and ΔP and ΔQ are related to each other by the expression $\Delta P/P = \Delta Q/Q$, one may transform formula (11) to new variables P and $\beta = \Delta P/P$. The old variables are related to the new ones as follows:

$$\begin{aligned} p_0 &= P(1+\beta) \\ q_0 &= (K^2\cos^2\theta - P^2)^{1/2}(1+\beta) \\ m_0 &= K\sin\theta(1 - 2\beta\cot^2\theta - \beta^2\cot^2\theta)^{1/2}. \end{aligned} \quad (13)$$

Formula (11) can be rewritten in the new variables as follows:

$$\psi_H = \int\int G' \exp\{i2\pi[Px + (K^2\cos^2\theta - P^2)^{1/2}y] \times (1+\beta)\}\, \mathrm{d}P\, d\beta. \quad (14)$$

Here $G' = K^2\cos^2\theta\ (K^2\cos^2\theta - P^2)^{-1/2}\ (1+\beta) \times G(P,\beta,\mathbf{R})$ and the function $G(P,\beta,\mathbf{R}) = G|\,p_0(P,\beta), q_0(P,\beta), \mathbf{R}\,|$ [see (11)]. Integration in (14) is carried out over the range $|P| \le K, |\beta| < 1$. G' is a slowly varying function of P. This allows us to evaluate the integral (14) over the variable P by the stationary-phase method:

$$\psi_H = \exp(-i\pi/4)\left[\frac{\cos^6\theta}{\lambda^6(x^2+y^2)}\right]^{1/4} \times \int_{|\beta|<1} G_{st} \exp[i2\pi K\cos\theta(x^2+y^2)^{1/2} \times (1+\beta)]\, \mathrm{d}\beta. \quad (15)$$

The function $G_{st} = G(P_{st},\beta,\mathbf{R})$ is calculated at the stationary-phase point: $P_{st} = Kx\cos\theta/(x^2+y^2)^{1/2}$.

We shall now find an explicit expression for $\psi_H(\mathbf{R})$ in the case of an ideal crystal plate of thickness t. The region corresponding to the volume v_c of the crystal is determined in the chosen coordinate system by the condition: $D_1 - t/2 \le \mathbf{n}_0.\mathbf{R}_c \le D_1 + t/2$, where $D_1 - t/2$ is the distance from the source to the entrance surface of the crystal.

In an ideal crystal the distribution $f(\mathbf{K}_h - \mathbf{K}_0)$ in the vicinity of the H point of the reciprocal lattice can be represented in the form

$$f_H = F_H\, \Omega^{-1} \int_{v_c} \exp(-i2\pi\Delta\mathbf{H}.\mathbf{R}_c)\, \mathrm{d}^3R_c. \quad (16)$$

Here Ω is the unit-cell volume, F_H is the structural amplitude for the H reflexion. For the considered crystal volume,

* A specific form of the distribution $f(\mathbf{K}_h - \mathbf{K}_0)$ for single crystals of various perfection, shape and dimensions was considered by many authors and described in a number of monographs (see James, 1948; Cowley, 1975).

$$f_H = \frac{tF_H}{\Omega \cos\alpha} \exp\left(-i2\pi \frac{D_1 \Delta H_z}{\cos\alpha}\right) \operatorname{sinc}\left(\frac{t\Delta H_z}{\cos\alpha}\right) \times \delta(\Delta H_y)\, \delta(\Delta H_x + \Delta H_z \tan\alpha).* \quad (17)$$

Using the relation $\mathbf{K}_h = \mathbf{K}_0 + \mathbf{H} + \Delta\mathbf{H}$, we substitute the integration over the variables p_h and q_h by that over ΔH_x and ΔH_y. In this case, the integration in (9) is carried out within the limits of the reciprocal-lattice-node section determined by (12). Using the conditions $|\Delta\mathbf{H}| \ll |\mathbf{H}|$ and $|\beta| \ll 1$, we obtain:

$$W_{st} = -i \frac{A_e C_s F_H \lambda t}{\Omega \gamma_H} \operatorname{sinc}\left(\frac{t\Delta H_z}{\cos\alpha}\right) \times \exp\{i2\pi[\mathbf{H}.\mathbf{R} + \Delta H_z(z - x\tan\alpha - D_1/\cos\alpha)]\}. \quad (18)$$

Here the factor C_s is equal to 1 or $\cos 2\theta$ for σ or π polarization, respectively; $\gamma_0 = \mathbf{s}_0^B.\mathbf{n}_0 = \sin\theta\cos\alpha - \lambda P_{st}\sin\alpha$ and $\gamma_H = \mathbf{s}_H^B.\mathbf{n}_0 = -\sin\theta\cos\alpha - \lambda P_{st}\sin\alpha$ are the cosines of the angles between the normal to the crystal surface $\mathbf{n}_0$ and the wave vectors $\mathbf{K}_0^B$ and $\mathbf{K}_H^B$, respectively;

$$\Delta H_z \simeq -\frac{2\cos^2\theta\cos\alpha}{\lambda\gamma_H} \times \left[\beta + \beta^2\left(\frac{\cos^2\theta}{\gamma_H^2} + \frac{\gamma_0\cos 2\theta}{2\gamma_H\sin^2\theta}\right)\right]. \quad (19)$$

* The function sinc is defined as $\operatorname{sinc}\xi = \sin(\pi\xi)/\pi\xi$, $\delta(\xi)$ is the Dirac function.

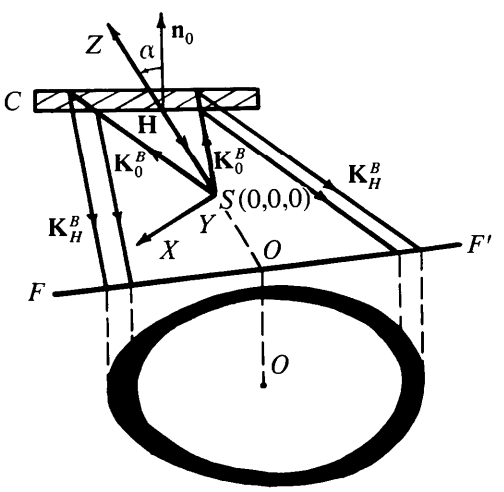

Fig. 2. Divergent-beam diffraction technique. S is the radiation source, C is the crystal, $\mathbf{n}_0$ is the normal to the crystal surface, FF' is the observation plane, XYZ is the coordinate system used.

The expression for $B(\beta,z)$ takes the form

$$B \simeq (i/K\sin\theta)\exp[i2\pi K|z|\sin\theta(1 - \beta\cot^2\theta - \beta^2\cot^2\theta/2\sin^2\theta)]. \quad (20)$$

In the phase factor we have kept terms up to the order of β^2.

Substituting the expressions for $G_{st} = BW_{st}$ into (15) and performing the change of variables $\eta = 2t\cos^2\theta \times \beta/\lambda\gamma_H$ we obtain:

$$\psi_H = A_e C_s F_H \lambda^{3/2}\cos^{1/2}\theta\,(\Omega\sin 2\theta)^{-1}(x^2+y^2)^{-1/4} \times \exp[i2\pi(\mathbf{K}_H^B.\mathbf{R} - 1/8)] \times \int_{-\infty}^{\infty} \operatorname{sinc}\eta\exp[i2\pi(\eta\Phi_H - \eta^2\lambda\tilde{R}\gamma_H^2/2t^2\sin^2 2\theta)]\,d\eta. \quad (21)$$

Here

$$\Phi_H = (2t)^{-1}[2D_1 + x\sin\alpha - z\cos\alpha + xz\sin\alpha\cot\theta(x^2+y^2)^{-1/2} - (x^2+y^2)^{1/2}\cos\alpha\tan\theta] \quad (22)$$

$$\tilde{R} = R_1 + R_2\gamma_H^{-2}(\sin^2 2\theta + 2\gamma_0\gamma_H\cos 2\theta - \gamma_H^2). \quad (23)$$

The distance R_1 is measured from the source to the crystal along the ray $\mathbf{K}_0^B$ and the distance R_2 is measured from the crystal to the observation point $\mathbf{R}$ along the ray $\mathbf{K}_H^B$. When $\mathbf{n}_0$ lies in the diffraction plane, (23) is simplified to $\tilde{R} = R_1 + R_2\gamma_0^2/\gamma_H^2$.

Formula (21) is equivalent to the expression describing plane-wave diffraction on a slit with the dimension $L = t\sin 2\theta/\gamma_H$ placed at a distance $\tilde{R}$ from the observation plane (Goodman, 1968).* The slit image centre is determined by the condition

$$\Phi_H = 0. \quad (24)$$

The value $L\Phi_H$ corresponds to the distance from the observation point to the image centre. Accordingly, in our case, (24) is an equation for the diffraction line centre (in the scattering plane) and determines a complex surface, which is described by a fourth-degree polynomial [see (22)]. The section of this surface by the film plane are recorded in the experimental set up.

We shall now analyse the integral in (21) and obtain an explicit expression for the distribution of diffraction line intensity.

4. The diffracted-wave intensity distribution

In the analysis of the diffraction pattern from a slit with dimension $L = t\sin 2\theta/\gamma_H$ placed at a distance $\tilde{R}$ from

* The situation is analogous to the case of normal incidence of a plane wave on the slit. Thereby the slit plane and the observation plane are considered parallel.

the observation plane one usually distinguishes three regions: the region of geometrical shadow image (I), the region of Fresnel diffraction (II) and that of Fraunhofer diffraction (III). The criteria for the observation plane to lie in one of these regions are

$$\begin{array}{cccc} & \text{region I} & \text{region II} & \text{region III} \\ & t \gg \sigma_F & t \sim \sigma_F & t \ll \sigma_l. \end{array} \qquad (25)$$

Here $\sigma_F = \delta_F \gamma_H / \sin 2\theta$, $\delta_F = (\lambda \tilde{R})^{1/2}$ is the dimension of the first Fresnel zone.†

At first glance, we have obtained an unusual result. An infinite crystal plate does not satisfy the Fraunhofer approximation conditions (3). However, at $t \ll \sigma_F$ such a plate gives the Fraunhofer diffraction pattern in the scattering plane just like a small crystal with dimension $l \ll (\lambda R^*)^{1/2}$. This fact follows from three-dimensional diffraction theory and can be explained in terms of a construction in reciprocal space. The reciprocal-lattice node for a thin plane parallel plate is extended only along one direction, therefore in spherical-wave diffraction on such a crystal only one diffracted plane wave is significant in expansion (4). As a result, the spectrum of diffracted waves corresponds to the distribution (10).

Let us determine the diffraction patterns for the different diffraction regions. In region I the condition $t \gg \sigma_F$ corresponds to the possibility of neglecting the term proportional to η^2 in the exponent in (21). In this case the integral is tabulated, and we can obtain the following expression:

$$\psi_H^{\mathrm{I}} = -\pi C_s \chi_H (\lambda R_0 \sin^2 2\theta)^{-1/2} \times \exp[i2\pi(\mathbf{K}_H^B . \mathbf{R} - 1/8)] \operatorname{rect} \Phi_H. \qquad (26)$$

Here $\chi_H = -A_e F_H \lambda^2 / \Omega$ is the Fourier expansion coefficient of the crystal polarizability, $R_0 = R_1 + R_2$, rect $\xi = 1$ at $|\xi| \leq 1/2$ and rect $\xi = 0$ at $|\xi| > 1/2$. The condition $|\Phi_H| \leq 1/2$ determines the shape and width of a diffraction line, $\Phi_H = 0$ corresponds to the centre [see (24)].

In region II the integral in (21) cannot be represented in analytical form. In region III the function sinc in the integrand of (21) may be considered as slowly varying in comparison with the oscillations of the exponent, and the main contribution to the integral comes from points in the vicinity of the stationary phase point. The calculations show that

$$\Psi_H^{\mathrm{III}} = i\pi C_s \chi_H t (\lambda \gamma_H)^{-1} (R_0 \tilde{R})^{-1/2} \operatorname{sinc}(t^2 \Phi_H / \sigma_F^2) \times \exp[i2\pi(\mathbf{K}_H^B . \mathbf{R} + t^2 \Phi_H^2 / 2\sigma_F^2)]. \qquad (27)$$

As in (26), the condition $\Phi_H = 0$ describes a locus corresponding to a diffraction line centre. For the rest, the distribution $\psi_H^{\mathrm{III}}(\mathbf{R})$ qualitatively differs from $\psi_H^I(\mathbf{R})$. In region I the diffraction lines have sharp edges (due to the function rect Φ_H), the line width is independent of the distances R_1 and R_2. In region III the distribution of intensity of a diffraction line is described by a smoothly varying function $\operatorname{sinc}^2(t^2 \Phi_H / \sigma_F^2)$, the diffraction line width is much larger than in region I, therefore this width increases with increasing R_1 and R_2. The integrated intensities do not depend on the diffraction regions (25) and are equal to*

$$I_H^{\mathrm{int}} = \int_{-\infty}^{\infty} |\psi_H|^2 \, \mathrm{d}(L \Phi_H) = (\pi C_s |\chi_H| t)^2 / \lambda R_0 \gamma_H \sin 2\theta. \qquad (28)$$

Integration in (28) is carried out in the scattering plane.†

We now compare formulae (26) and (27) with some known results. In the scattering plane, containing a normal to the crystal plate surface, (26) corresponds to the limiting transition $t/\Lambda_H \ll 1$ in the dynamical theory developed by Kato (1961)‡ and (27) can be obtained in the limits $t/\Lambda_H \ll 1$ and $t/\sigma_F \ll 1$, using the dynamical theory developed by Afanas'ev & Kohn (1977).§ In the case of Bragg symmetric diffraction and $R_1 \gg R_2$, formula (27) gives an expression, known in kinematical theory, for the reflexion coefficient of an X-ray wave emitted by a point source and reflected by an atomic plane. This expression has been obtained by Darwin, using the method of summation of Fresnel zone contributions (see James, 1948):

$$|q| = A_e C_s |F_H| d_H \lambda / \Omega \sin \theta. \qquad (29)$$

Formula (27) also includes another known expression for the intensity of a wave scattered by a crystal plate with thickness Nd_H:

$$I(\varepsilon) = |q|^2 N^2 \operatorname{sinc}(2\varepsilon d_H N \cos\theta / \lambda) \qquad (30)$$

provided the incident wave amplitude is equal to 1 on the crystal surface (see James, 1948). In (30) $\varepsilon = L\Phi_H / \tilde{R}$ is the deviation from the Bragg angle θ. Thus, (26) and (27) contain known results or agree with them.

Based on the above-mentioned results, one can arrive at the following conclusion. The form of intensity distribution depends on the observation conditions and has distinctive features in different regions of observation (25). This means that the problem of determining the form of a reciprocal-lattice node from the intensity distribution involves solving the convolution equation and cannot have an unambiguous answer without involving additional information on the crystal itself.

Note 1. In a real experiment the diffraction pattern is obtained by summing the waves scattered by different blocks of the crystal mosaic. Mosaic blocks are

† δ_F is equal to 3 μm for $\lambda = 1$ Å and $\tilde{R} = 10$ cm. This means that the experimental diffraction pattern may correspond to any of the regions I, II or III.

* This result follows also from the Parseval theorem.

† For unpolarized radiation $C_s = (1 + \cos^2 2\theta)/2$.

‡ Λ_H is the extinction distance.

§ See also Aristov, Afanas'ev, Kohn & Polovinkina (1980).

infinitesimal elements of a large object – the crystal. Therefore, when the applicability of various approximations is estimated, one should take into account not only the dimensions of the infinitesimal elements, but the dimensions of the whole object as well. Taking this into account conditions (25) can be rewritten:

$$\begin{array}{lll} \text{region I} & \text{region II} & \text{region III} \\ t \gg \sigma_F & t \lesssim \sigma_F \lesssim (tT)^{1/2} & (tT)^{1/2} \ll \sigma_F. \end{array} \quad (31)$$

Here t is the mosaic block thickness, T is the crystal thickness. It follows from (31) that in spherical-wave diffraction by a crystal of large dimensions the diffraction pattern, as a rule, is not Fraunhofer's, even if the crystal consists of fine blocks.

Note 2. Above, we have ascertained that the diffraction pattern geometry (the shape and position of diffraction lines on the X-ray pattern) is independent of the diffraction region in which the observation plane is located. Using the dynamical approximation of the theory, one may show that the diffraction pattern geometry in this case can be also described in terms of sections of the surface $\Phi_H = 0$ (within the corrections for X-ray refraction and absorption in the crystal). This conclusion is of great importance for a practical application of the DB and PK methods to the investigation of single-crystal structures.

The problem of describing the DB diffraction pattern geometry has been solved by many authors by determining the paths of the rays diffracted by the crystal at the Bragg angle. Since the relation $R_2 \gg R_1$ is satisfied in the PK scheme, such diffracted patterns are satisfactorily interpreted in terms of conic sections, similarly to the Kossel lines, and have been studied in detail (see Tixier & Wache, 1970). In the DB scheme R_2 is greater than or close to R_1, and diffraction lines may appreciably differ from second-order curves (Imura, Weissmann & Slade, 1962; Newman, 1970; Vasil'ev & Ivanov, 1971). As a consequence, the DB diffraction pattern is more complicated and has not been described in detail up to now.* Therefore it should be of interest to analyse in detail the diffraction pattern geometry, and determine the dependence of the diffraction line shape on the orientation of the reflecting planes and the experimental geometry.

5. Diffraction pattern geometry

In order to analyse the section of the diffraction surface $\Phi_H = 0$ with the observation plane $\mathbf{n}_0 . \mathbf{R} = D_2$, we use a new coordinate system $X_1Y_1Z_1$ in which the Z_1 axis is parallel to the normal $\mathbf{n}_0$. For that, we turn the old coordinate system XYZ about the Y axis by the angle $-\alpha$. Therefore the variables x,y,z are replaced by $x = x_1 \cos\alpha - z_1 \sin\alpha$, $y = y_1$, $z = x_1 \sin\alpha + z_1 \cos\alpha$. In the $X_1Y_1Z_1$ system the entrance and exit surfaces of the crystal are described by the equations $z_1 = D_1 - t/2$ and $z_1 = D_1 + t/2$, respectively. The equation $z_1 = D_2$ is determined by the observation plane.

In the $X_1Y_1Z_1$ system (24) can be rewritten for the case $|\alpha| = \pi/2$ as follows:

$$(2D_1 - D_2)(D_2^2 + y_1^2)^{1/2} - x_1 D_2 \cot\theta \operatorname{sgn}\alpha = 0.* \quad (32)$$

For the case $|\alpha| \neq \pi/2$ we also introduce the coordinate system X_2Y_2, which corresponds to a parallel translation of the system $X_1Y_1Z_1$ from point S to point O: $x_2 = x_1 - D_2 \tan\alpha$, $y_2 = y_1$ (see Fig. 3). In the X_2Y_2 system (24) takes the form

$$(2D_1 - D_2)(x_2^2 \cos^2\alpha + y_2^2)^{1/2} + x_2 D_2 \sin\alpha \cot\theta + x_2^2 \sin^2\alpha \cos\alpha \cot\theta - (x_2^2 \cos^2\alpha + y_2^2)\cos\alpha \tan\theta = 0. \quad (33)$$

The solution of (33) may be represented in the form

$$r(\varphi) = \frac{\cos\theta}{\cos\alpha}\left[\frac{D_1}{\sin(\theta - \theta_1)} + \frac{D_1 - D_2}{\sin(\theta + \theta_1)}\right], \quad (34)$$

where $\theta = \arcsin(\sin\alpha \cos\varphi)$, r and φ are polar coordinates of point M on a diffraction line ($x_2 = r\cos\varphi, y_2 = r\sin\varphi$).†

Before proceeding to a consistent analysis of the expressions obtained, we concentrate our attention on the most general features of diffracted lines that can be directly drawn from the properties of (32) to (34).

* The function sgn ξ is equal to 1 for $\xi > 0$, 0 for $\xi = 0$, -1 for $\xi < 0$.

† Expression (34) coincides with the formula we have derived by determining the path of rays diffracted by the crystal (Aristov, Shmyt'ko & Shulakov, 1974). In the particular case $D_2 = 0$ (33) and (34) coincide with equations obtained by Newman (1970).

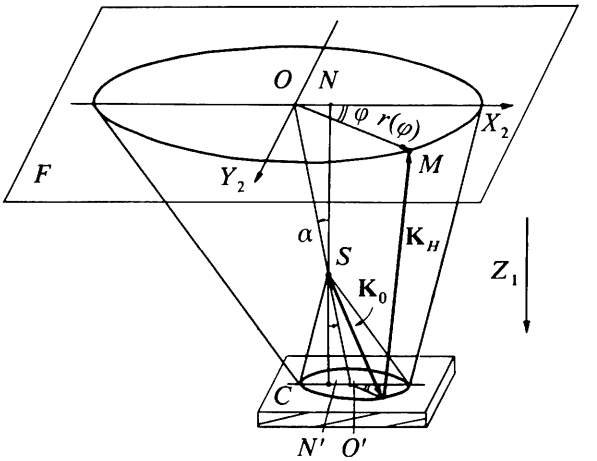

Fig. 3. Picture clarifying the choice of the coordinate system X_2Y_2. S is the source, C is the crystal, F is the film. Line OO' is parallel to the normal to the reflecting planes, NN' is the perpendicular to the crystal surface, $SN' = D_1 - t/2$, $SN = |D_2|$.

* Special features of the optical diffraction scheme with the DB method are considered in a paper by Aristov, Shektman & Shmyt'ko (1976).

1. All diffraction lines are symmetric relative to the X axis. The lines corresponding to the angles α and $-\alpha$ have an identical shape.

2. At $\alpha \neq 0$ and $|\alpha| \neq \pi/2$ a line shape is described by a fourth-degree polynomial. The line equations are simplified in the planes $z_1 = 0$, $z_1 = D_1$ and $z_1 = 2D_1$. The lines acquire a centre of symmetry in the plane $z_1 = 0$ containing the radiation source. The diffraction lines at $D_2 = D_1$ and $D_2 = 2D_1$ are second-order curves.

3. The diffraction lines at $\alpha = 0$ take the form of a circumference with the radius $r = (2D_1 - D_2)\cot\theta$. The lines at $|\alpha| = \pi/2$ are second-order curves, and in the plane $z_1 = 2D_1$ are straight ones.

Equations (32) to (34) describe both real and imaginary diffraction lines. The latter ones correspond to a continuation of the diffraction surface in the region of imaginary sources. Real diffraction lines are curves satisfying the conditions $\gamma_0 > 0$ and $\gamma_H > 0$ for the forward reflexion observation planes ($D_2 > D_1$) or $\gamma_0 > 0$ and $\gamma_H < 0$ for those in back-reflexion ($D_2 < D_1$). The condition $\gamma_0 > 0$ corresponds to the case of the incident wave propagating towards the crystal; the condition $\gamma_H > 0$ corresponds to the Laue case, and the condition $\gamma_H < 0$ to the Bragg case of diffraction. Let us write the expressions for γ_0 and γ_H. At $|\alpha| \neq \pi/2$:

$$\gamma_0 = \cos\alpha\sin(\theta - \theta_1)/\cos\theta_1$$
$$\gamma_H = -\cos\alpha\sin(\theta + \theta_1)/\cos\theta_1. \qquad (35)$$

At $|\alpha| = \pi/2$:

$$\gamma_0 = \gamma_H = D_2\cos\theta/(D_2^2 + y_1^2)^{1/2}. \qquad (36)$$

To analyse a line shape, it is convenient to separate the angular range of α ($-\pi < \alpha \leq \pi$) into four regions: in the first $|\alpha| < \theta$ and $|\alpha| > \pi - \theta$, in the second $|\alpha| = \theta$ and $|\alpha| = \pi - \theta$, in the third $\theta < |\alpha| < \pi/2$ and $\pi/2 < |\alpha| < \pi - \theta$, and in the fourth $|\alpha| = \pi/2$. The values of α satisfying the condition $|\alpha_1 - \alpha_2| = \pi$ correspond to diffraction by a single system of reflecting planes hkl and $\bar{h}\bar{k}\bar{l}$, and therefore are considered simultaneously. Below, such reflexions will be denoted as H (if $-\pi/2 < \alpha \leq \pi/2$) and $\bar{H}$ in the other cases.

(a) The case of $|\alpha| < \theta$ *and* $|\alpha| > \pi - \theta$

For $|\alpha| < \theta$ (the H reflexion) $\gamma_0 > 0$ and $\gamma_H < 0$; for $|\alpha| > \pi - \theta$ (the $\bar{H}$ reflexion) the diffraction conditions are not satisfied ($\gamma_{\bar{0}} < 0$). The lines for which $|\alpha| < \theta$ are recorded only on the back-reflexion pattern. All the lines are closed. Their shape, as a rule, is oval. While passing through the plane $z_1 = 0$, the major axis of the oval reverses its direction. The closed diffraction lines are usually like ellipses. However, when the angle $|\alpha|$ becomes close to θ, inflection points appear on the lines. The range of α and θ values, for which a change of the sign in the line curvature is observed, depends on the distance D_2. Thus, in the plane $z_1 = 0$ the region under consideration is limited by the inequalities:

$$\sin^2\theta/(1 + \sin^2\theta) < \sin^2\alpha < \sin^2\theta. \qquad (37)$$

Fig. 4 presents the change of line shape for different values of α. In the limiting cases $D_1 - D_2 \gg D_1$ or $0 < D_1 - D_2 \ll D_1$ all the closed lines may be regarded as ellipses.

(b) The case of $|\alpha| = \theta$ *and* $|\alpha| = \pi - \theta$

For $|\alpha| = \theta$ specific features related to the behaviour of the parameters γ_0 and γ_H are observed on the diffraction curves. Thus, the condition $\gamma_0 > 0$ is satisfied only for the angles $\varphi \neq \varphi_c = \arccos(\operatorname{sgn}\alpha)$. For $\varphi = \varphi_c$ the value γ_0 is equal to zero and the diffraction conditions for the incident wave are not realized. In addition, at $\varphi = \pi - \varphi_c$, $\gamma_H = 0$ and the diffracted ray direction becomes parallel to the crystal surface. At other angles φ, γ_H is negative. This corresponds to Bragg diffraction. The features mentioned above result in $r \to \infty$, as $\varphi \to 0$ or $\varphi \to \pi$, *i.e.* the diffraction lines are no longer closed. Fig. 5 presents the shape of the diffraction lines corresponding to the condition $|\alpha| = \theta$ for different values of D_2. Each of these lines consists of two branches situated symmetrically relative to the X axis. The lines under consideration are typical fourth-order curves and are not interpreted in terms of conic sections for any D_2, including the case $D_1 - D_2 \gg D_1$. Also note that these are curves of varying curvature. The diffraction condition $\gamma_{\bar{0}} > 0$ is not realized for the $\bar{H}$ reflexion.

(c) The case of $\theta < |\alpha| < \pi/2$ *and* $\pi/2 < |\alpha| < \pi - \theta$

For such an α the values $\gamma_0 = \gamma_{\bar{H}}$ and $\gamma_H = \gamma_{\bar{0}}$ equal zero when $\varphi = \varphi_{1,2} = \pm\arccos(\sin\theta/\sin\alpha)$ and $\varphi =$

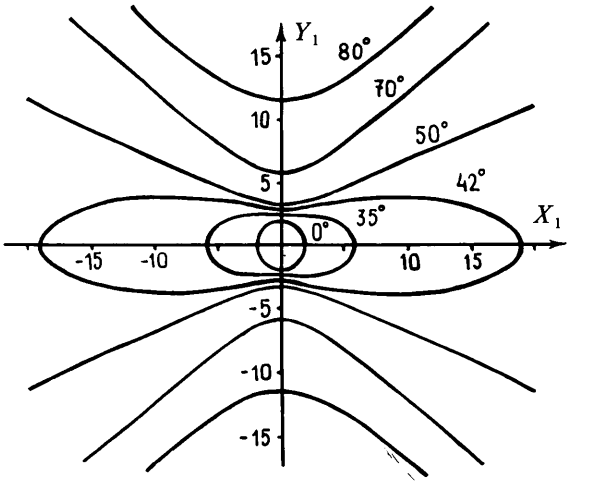

Fig. 4. Diffraction pattern geometry in the plane $z_1 = 0$; the zone axis for reflecting planes is parallel to the Y axis. The curves are constructed for $D_1 = 1$, $\theta = 45°$ and the angle α is equal to 0, 35, 42, 50, 70 and 80°. The condition $\alpha < 45°$ corresponds to closed lines; when $35°\,16' < \alpha < 45°$ curves of varying curvature are obtained.

$\varphi_{3,4} = \pi \mp \arccos(\sin\theta/\sin\alpha)$, respectively. The half-straight lines defined by these angles φ_1, φ_2, φ_3 and φ_4 separate the plane X_2Y_2 into the regions in which different combinations of signs of γ_0 and γ_H or γ_0 and $\gamma_{\bar{H}}$ are realized. All the lines observed are open ($r \to \infty$, as $\varphi \to \varphi_i$, $i = 1, 2, 3, 4$). To analyse these lines, we consider a section of the diffraction surface by the plane $z_1 = D_1$ (see Fig. 6).* The H and $\bar{H}$ curves are the branches of a hyperbola and correspond to the crystal points satisfying the Bragg reflection conditions. It follows from (35) that the H branch is completely situated in the Laue diffraction region ($\gamma_{\bar{H}} > 0$) and that it corresponds to the lines on the transmission patterns ($D_2 > D_1$). The H branch along the segments ∞a and $b\infty$ lies in the Bragg diffraction region ($\gamma_H < 0$, $D_2 < D_1$), and along the segment ab in the Laue region ($\gamma_H > 0$, $D_2 > D_1$). Division of the H branch into the segments of the Laue and Bragg cases of diffraction leads to the appearance of diffraction lines both in the back-reflexion and transmission scheme (from the segments $a\infty$ and $b\infty$, and the segment ab, respectively).

Fig. 7 presents the diffraction lines recorded in the back-reflexion scheme at different distances $D_2 < D_1$. In the planes located near the crystal surface ($0 < D_1 - D_2 \ll D_1$) the diffraction line shape approaches a curve formed from the segments ∞a and $b\infty$ of the H branch of the hyperbola (see Fig. 6) and the rays aa' and bb' corresponding to the condition $\gamma_H = 0$. The upper and lower branches of the described diffraction lines have different asymptotes and, consequently, are not hyperbolae in any plane $z_1 = \text{constant}$.

Now consider the transmission case. Fig. 8 presents the form of the diffraction curves in different planes $z_1 = D_2 > D_1$ for the H and $\bar{H}$ reflexions. At the distance D_2 satisfying the condition:

$$D_2/D_1 - 1 < \sin^2(\theta - \alpha)/\sin^2(\theta + \alpha) < 1, \quad (38)$$

the branch H is a curve of a varying curvature. At $D_2 = 2D_1$ the branches H and $\bar{H}$ coincide. With further increase of D_2 the branches H and $\bar{H}$ change place. At distances D_2 satisfying the condition

$$1 < \sin^2(\theta - \alpha)/\sin^2(\theta + \alpha) < D_2/D_1 - 1, \quad (39)$$

* The diffraction lines presented in Figs. 6 to 8 correspond to the reflexions $\bar{1}\bar{1}3$ ($\alpha = 79°\,58'$, H reflexion) and $11\bar{3}$ ($\alpha = -100°\,2'$, $\bar{H}$ reflexion) for a Si single crystal with the surface plane (111), Cu $K\alpha$ radiation ($\theta \simeq 28°$), $D_1 = 1$. In our notation $\varphi_a = \arccos(\sin\theta/|\sin\alpha|)$.

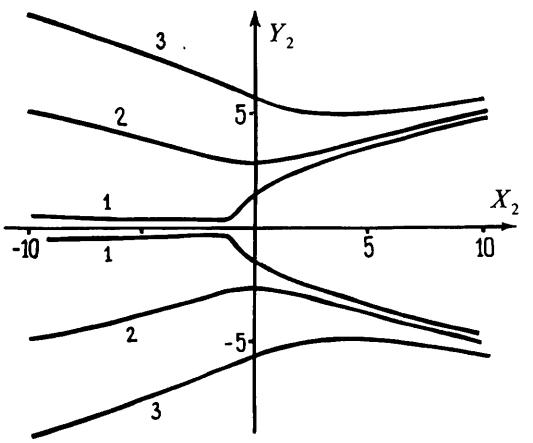

Fig. 5. Diffraction lines corresponding to the condition $|\alpha| = \theta$. The curves are constructed for $D_1 = 1$, $\alpha = \theta = 45°$. The distance D_2 is equal to 0·99 (curve 1), 0 (curve 2), −1 (curve 3).

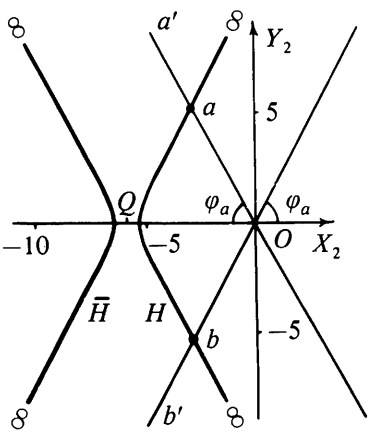

Fig. 6. Intersection of the diffraction surfaces $\Phi_H = 0$ and $\Phi_{\bar{H}} = 0$ with the observation plane $z_1 = D_1$. Point Q is the centre of the hyperbola, $\varphi_a \simeq 61°$.

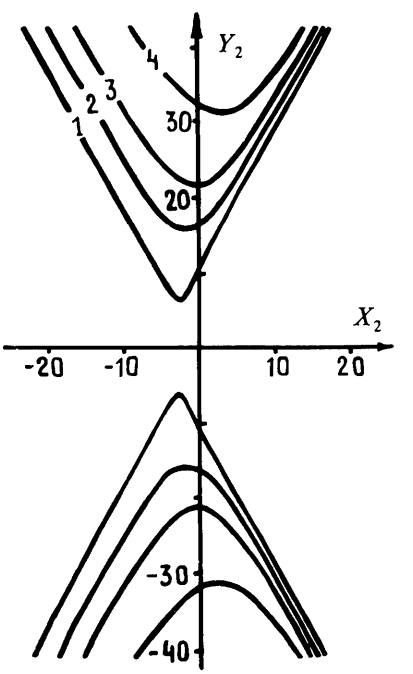

Fig. 7. Diffraction lines corresponding to the condition $\theta < |\alpha| < \pi/2$ and recorded in the back-reflexion scheme. Curves 1, 2, 3, 4 are constructed for distances D_2 equal to 0·99, 0·5, 0, −1.

the branch $\bar{H}$ is a curve of varying curvature. For $D_2 \gg D_1$ in the range of angles φ which are not too close to φ_i, the branches H and $\bar{H}$ are branches of a hyperbola.

(d) The case of $|\alpha| = \pi/2$

The diffraction lines at $|\alpha| = \pi/2$ are observed only in the transmission scheme and are hyperbolae in the planes $z_1 = D_2 \neq 2D_1$. At $D_2 = 2D_1$ the branches H and $\bar{H}$ coincide and degenerate into a straight line [see (32)]. When the normal to the crystal surface n_0 coincides with the zone axis, the diffraction pattern on the X-ray photograph located in the plane $z_1 = 2D_1$ looks like a fan of straight lines passing through the point $x_1 = 0$ and $y_1 = 0$ and corresponding to the directions of crystallographic symmetry (see Fig. 9).

Note 1. The intensity of the diffraction line recorded on the film parallel to the crystal surface is determined by the expressions: $J_H(\mathbf{R}) = |\gamma_H(\mathbf{R}|\,|\psi_H(\mathbf{R})|^2$, where $J_H(\mathbf{R})$ is the illumination intensity at the observation point $\mathbf{R}$. In regions I and III the distribution $J_H(\mathbf{R})$ can be represented in explicit form:

$$J_H^{\mathrm{I}} = \pi^2 C_s^2 |\chi_H|^2 (\gamma_H/\lambda R_0 \sin^2 2\theta) \operatorname{rect} \Phi_H \quad (40)$$

$$J_H^{\mathrm{III}} = \pi^2 C_s^2 |\chi_H|^2 (t^2/\lambda R_0 \bar{R} \gamma_H) \operatorname{sinc}^2 (t^2 \Phi_H/\sigma_F^2). \quad (41)$$

The values γ_0 and γ_H are determined by (35) and (36),

$$R_0 = D_1 \gamma_0^{-1} + (D_2 - D_1)\gamma_H^{-1}$$

$$\bar{R} = D_1 \gamma_0^{-1} + (D_2 - D_1)\gamma_H^{-3} \times (\sin^2 2\theta + 2\gamma_0 \gamma_H \cos 2\theta - \gamma_H^2). \quad (42)$$

It is seen from (40) and (41) that the intensity $J_H(\mathbf{R})$ at $\alpha \neq 0$ changes along a diffraction line (as φ changes). The line segments for which $\gamma_0 \simeq 0$ or $\gamma_H \simeq 0$ correspond to zero intensity and, consequently, are not recorded on the X-ray photograph. The lines (or line segments) for which the values γ_0 and γ_H are of the order of 1 have the highest intensity. This condition corresponds to the centre of the X-ray pattern.

Let us concentrate our attention on the fact that (40) and (41) depend on the parameters γ_0 and γ_H in a nonsymmetric way. This means that some asymmetry of intensity for the segments of the diffraction lines corresponding to $\gamma_0 \to 0$ or $\gamma_H \to 0$ (at $\gamma_0 \to 0$, $J_H^{\mathrm{I}} \sim \gamma_0$ and $J_H^{\mathrm{III}} \sim \gamma_0^2$; at $\gamma_H \to 0$, $J_H^{\mathrm{I}} \sim \gamma_H^2$ and $J_H^{\mathrm{III}} \sim \gamma_H^3$) should be clearly observable for the open lines in the Bragg diffraction case (see Fig. 7). Such lines often appear on the X-ray patterns obtained at distances $D_1 - D_2$ much smaller than the film dimensions (see Fig. 10). The symmetric sections of some lines are not recorded on the film because their intensity is too weak.

It also follows from (35), (36) and (42) that the parameter σ_F changes along a diffraction line at $\alpha \neq 0$. This means that different segments of a line may

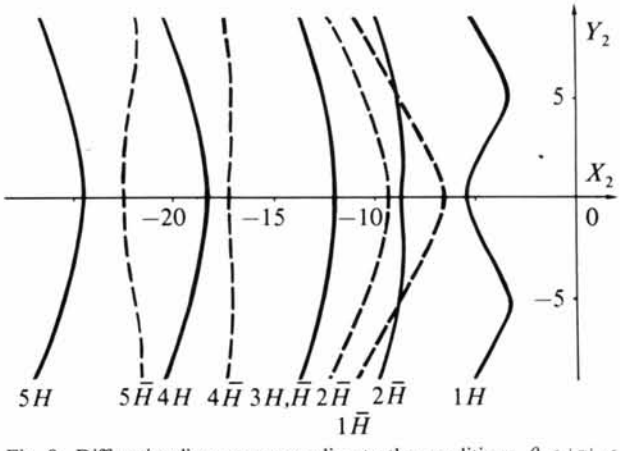

Fig. 8. Diffraction lines corresponding to the conditions $\theta < |\alpha| < \pi/2$ and $\pi/2 < |\alpha| < \pi - \theta$ and recorded with the transmission technique. Curves 1, 2, 3, 4, 5 are constructed for the distances D_2 equal to 1·01, 1·5, 2, 3, 4.

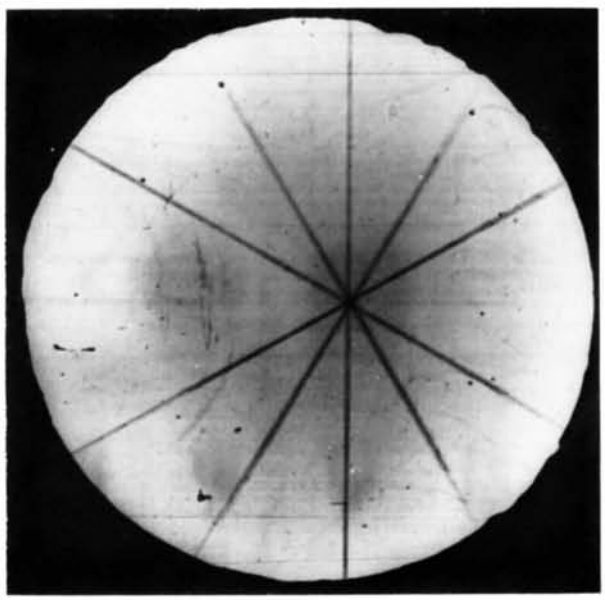

Fig. 9. The X-ray pattern of an Al_2O_3 crystal recorded at the distance $D_2 = 2D_1$, by making use of a screen protecting the observation region from the transmitted beam. The normal to the crystal surface coincides with the direction [111]; radiation Cu $K\alpha$.

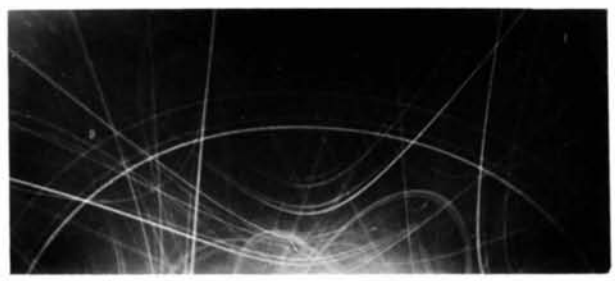

Fig. 10. X-ray pattern from a fragment of Si crystal recorded in the back-reflexion scheme. Surface plane (111), radiation Cu $K\alpha$.

correspond to different diffraction regions and hence different intensity distributions [see (40) and (41)]. At $\gamma_0 \to 0$ or $\gamma_H \to 0$ σ_F tends to zero, and the case of Fraunhofer diffraction is realized.

Note 2. The width of diffraction lines is determined by the conditions $|\Phi_H| \leq 1/2$ (in region I) or $|\Phi_H| \lesssim \sigma_F^2/t^2$ (in region III). Without going into a detailed analysis of these relations, it is worth mentioning that the diffraction line width at $\alpha \neq 0$ is not constant and may vary over a wide range.

4. The diffraction lines recorded with the divergent-beam technique correspond to intersections of surfaces $\Phi_H = 0$ with the observation plane and are fourth-order curves. The line shapes are of a wide variety and include both closed and open lines, curves with a varying curvature, *etc.* The width and intensity of the diffraction lines are not constant at $\alpha \neq 0$ and may vary over a wide range.

Conclusion

The basic results of this paper are the formulation of a kinematical theory of spherical X-ray wave diffraction and the analysis of the diffraction pattern from a thin perfect crystal. The expressions obtained describe both shape and structure (intensity distribution in the scattering plane) of the diffraction lines recorded on the X-ray photographs for any geometry of experiment. The investigations carried out enable us to draw the following conclusions.

1. In the crystal diffraction of a spherical X-ray wave, the Fraunhofer diffraction conditions are not valid for a wide variety of single crystals with different degrees of perfection. This can be applied to the divergent beam and pseudo-Kossel techniques.

2. The intensity distribution of the diffracted wave essentially depends on the region in which the observation plane is located. Region (I) pertains to diffraction of a geometrical shadow image, regions (II) and (III) correspond to Fresnel and Fraunhofer diffraction, respectively. In regions I and II an interpretation of the diffracted wave intensity distribution in terms of the intersections of reciprocal-lattice nodes with the Ewald sphere is incorrect.

3. The diffraction pattern geometry is determined only by the crystal structure and the geometry of the experiment and is independent of the diffraction region in which the observation plane is located.

References

AFANAS'EV, A. M. & KOHN, V. G. (1977). *Fiz. Tverd. Tela*, **19**, 1775–1783.

ARISTOV, V. V., AFANAS'EV, A. M., KOHN, V. G. & POLOVINKINA, V. I. (1980). *Acta Cryst.* A**36**, 1002–1013.

ARISTOV, V. V., SHEKTMAN, V. SH. & SHMYT'KO, I. M. (1976). *Kristallografiya*, **21**, 50–56.

ARISTOV, V. V., SHMYT'KO, I. M. & SHULAKOV, E. V. (1974). *J. Appl. Cryst.* **7**, 409–413.

BORN, M. & WOLF, E. (1968). *Principles of Optics.* New York: Pergamon Press.

COWLEY, J. M. (1975). *Diffraction Physics.* Amsterdam, Oxford: North-Holland.

GOODMAN, J. W. (1968). *Introduction to Fourier Optics.* New York: McGraw-Hill.

IMURA, T., WEISSMANN, S. & SLADE, J. J. (1962). *Acta Cryst.* **15**, 786–793.

IVERONOVA, V. I. & REVKEVICH, G. P. (1978). *Theory of X-ray Scattering* (in Russian). Moscow: Moscow State Univ.

JAMES, R. W. (1948). *The Optical Principles of the Diffraction of X-rays.* London: Bell.

KATO, N. (1961). *Acta Cryst.* **14**, 526–533, 627–636.

NEWMAN, B. A. (1970). *J. Appl. Cryst.* **3**, 191–193.

SAMSONOV, V. M. (1979). *On Specific Features of X-ray Spherical Wave Diffraction on Perfect Crystals of Finite Dimensions* (in Russian). Preprint of Nuclear Physics Institute, Leningrad.

TIXIER, R. & WACHE, C. (1970). *J. Appl. Cryst.* **3**, 466–485.

VASIL'EV, D. M. & IVANOV, S. A. (1971). *Zavod. Lab.* **37**, 1099–1103.